Topological transition in dynamic complex networks

Nobuharu Kami[1,2,*] and Hideo Ikeda[1,3,†]
[1]*Department of Electrical Engineering, Stanford University, Stanford, California 94305–9510, USA*
[2]*System Platforms Research Laboratories, NEC Corporation, Kawasaki 211–8666, Japan*
[3]*Production Systems Research Laboratory, Kobe Steel, Ltd., Kobe 651–2271, Japan*
(Received 10 September 2008; revised manuscript received 6 March 2009; published 22 May 2009)

Using a network model involving statistical mechanics we study the topological transition of complex networks with evolving wiring structure. The evolution rule of our network model contains both a structuring effect originated in a wiring decision metric (local clustering coefficient) and a randomizing effect due to thermal fluctuation. Monte Carlo simulation results show a dramatic topological transition between nonclustered networks and clustered networks in response to changes in the degree of randomness.

DOI: 10.1103/PhysRevE.79.056112 PACS number(s): 89.75.Fb, 64.60.De, 64.60.Cn, 64.60.aq

I. INTRODUCTION

The pattern of connections in networked systems such as computer networks, biological networks, and social networks is a topic of great interest to researchers in a variety of fields. High-level abstraction and modeling is an effective way of analyzing the mechanism of evolution and predicting the behavior of such networks. Many network models have been proposed for discussing why and how the connection patterns emerge and what properties the networks have. Most of these networks have no central control for the wiring-configuration generation rules. Each vertex autonomously makes its own decision about the wiring configuration and the resulting topologies often contain a very complex structure.

Random graphs were first studied by Erdos and Renyi [1–3]. Although their models are simple tools that reveal a lot of interesting average properties, many real networks such as World Wide Web (WWW) hyperlink networks and social networks have different properties from those of random graphs. Consequently, many other models have been proposed over the years. For example, Watts and Strogatz [4,5] proposed a simple model for producing small world networks [6] that have a highly clustered topology yet a small degree of separation between all vertices. Barabasi and Albert [7] proposed the BA model, which contains two properties, network growth and preferential attachment, to explain why the degree distribution of WWW networks follows a power-law distribution. These models help us understand the basic properties of such networks and many other models have been derived from them. For more extensive information regarding recent work on the models of complex networks, readers should refer to [8–12].

Most of these models locally define random process for updating the network's wiring configuration, and each vertex is given a metric for making wiring decisions. The main interest is to learn the topology or other important network properties such as the clustering coefficient and the average shortest path length of the networks generated through the generation process.

However, it is also important to study the equilibrium states that a system reaches after repetitions of local wiring updates according to an evolution rule that contains both structuring and randomizing effects in the wiring decision. In particular, when vertices dynamically interact with each other in making next wiring decisions, complex interaction patterns of the wiring update decisions appear and cause a lot of interesting phenomena similar to the phase transition observed in Ising model or spin glasses [13]. In order to analyze the rich phenomena, it is important to construct a model that formalizes such network-evolution process and observe the equilibriums resulting from competition between structuring and randomizing effects.

In this study, we devised a model involving statistical mechanics for studying the equilibrium states of the network evolution where vertices keep updating the configuration of the incoming edges by taking a clustering coefficient, one of the most important measures of complex networks, as an evolution metric. As we will show, our model uses the concept of temperature to express the degree of randomness in wiring decisions. We show that the transition between nonclustered and clustered topologies is observed in response to changes in the degree of randomness. We also discuss how complex interaction patterns form by analyzing the results of a damage-spreading simulation and by devising a percolation expression applicable to our model.

II. MODEL DESCRIPTION

Suppose that a network contains N vertices, and each vertex autonomously selects K different vertices as its "friends" to ask for some information by creating directed edges. Our goal is to provide a model for observing the temporal evolution of this network and, in particular, the resulting topological structure of the network in its equilibrium states. To this end, we define a network model and evolution rules as follows.

A. Definitions

1. State space

Throughout this paper, we consider the following set of directed graphs Σ as the state space of the system:

*n-kami@ak.jp.nec.com
†ikeda.hideo@kobelco.com

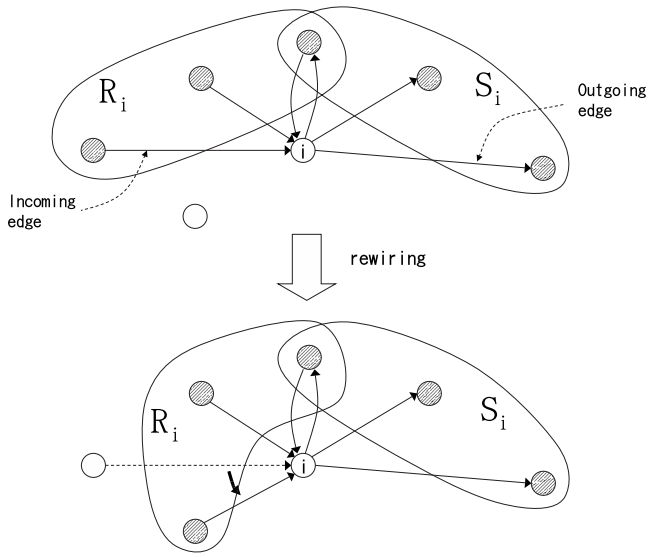

FIG. 1. Illustration of incoming and outgoing adjacent vertices.

$$\Sigma = \{g = (V,E) | |V| = N, |E| = NK, (N,K \in \mathbb{N})\}. \quad (1)$$

Here, $|X|$ denotes the number of elements of set X. A configuration g, which is an element of Σ, specifies a certain wiring configuration, and it can also be mapped to an adjacency matrix A in a one-to-one manner. The entry a_{ij} of the adjacency matrix A is defined by

$$a_{ij} = \mathbf{1}_{\{(i,j) \in E\}}, \quad (2)$$

where $\mathbf{1}_{\{statement\}}$ is the indicator function that returns 1 when *statement* is true and 0 otherwise. Note that we define a direction of edges such that it represents information flow. For example, creation of an edge $e=(j,i) \in E$ represents that vertex i makes a reference to vertex j.

2. Adjacent vertex sets

We also define R_i and S_i $\forall i \in V$ as follows:

$$R_i = \{j | \forall j \in V, j \neq i, (j,i) \in E\}, \quad |R_i| = K, \quad (3)$$

$$S_i = \{j | \forall j \in V, j \neq i, (i,j) \in E\}, \quad |S_i| \leq N - 1. \quad (4)$$

R_i is a set of vertices whose outgoing edges are connected to vertex i (vertices to which vertex i chooses to have a connection), while S_i is a set of vertices whose incoming edges are connected to vertex i (vertices which chose to connect to vertex i) as shown in Fig. 1. The set $R_i \cup S_i$ denotes the set of all adjacent vertices of vertex i, whereas $R_i \cap S_i$ denotes the set of vertices having mutual references with vertex i.

3. Restrictions

Throughout the evolution, each vertex has a fixed number of incoming edges (K edges). Thereby the number of 1's of all columns of all possible adjacency matrices is strictly K in our model. In addition, all vertices are allowed to directly change only their incoming edges configuration. We also prohibit self-reference and double reference (multiple edges between the same pair of vertices),

$$i \neq j \quad \forall (i,j) \in E, \quad (5)$$

$$e \neq e' \quad \forall e,e' \in E. \quad (6)$$

This means that the diagonal entries of all possible adjacency matrices in the state space are 0 and other entries are either 0 or 1.

B. Evolution rules and equilibriums

The network evolves in such a way that each vertex keeps being chosen among V in a round-robin manner and given a chance for rewiring. When vertex i is chosen, it acts as follows:

Step 1—Vertex i randomly picks one vertex ($a \in R_i$) among the incoming adjacent vertices and a new vertex ($b \in V \backslash R_i$) among all vertices minus the vertices in the set of incoming adjacent vertices.

Step 2—It compares b to a according to a given metric and replaces a with b with a certain probability.

This state transition corresponds to randomly selecting a pair of 1 and 0 in column i of the adjacency matrix and swapping them with a certain transition probability. Repetition of this rewiring at each vertex is represented by a series of state transitions in the state space, $g(t) \to g(t+1) \to g(t+2) \to \cdots$.

In order to get the transition probability from one state to another, we take advantage of the statistical-mechanics approach [13] and define a real-valued function on Σ, the Hamiltonian of the system $\mathcal{H}(g)$, which is interpreted as an energy of the system when in the configuration g.

In statistical mechanics, Gibbs' measure, which is the probability of the network having a configuration g after the system has reached equilibrium, is given by

$$G(g,\beta) = \frac{\exp\{-\beta \mathcal{H}(g)\}}{Z(\beta)}, \quad (7)$$

where $Z(\beta)$ is the partition function given by

$$Z(\beta) = \sum_{g \in \Sigma} \exp\{-\beta \mathcal{H}(g)\}. \quad (8)$$

According to the Metropolis method [14], the state transition probability from the state g to the state h is given by

$$\mathbf{Pr}\{g \to h\} = \min\left\{1, \frac{G(h)}{G(g)}\right\} = \min\{1, \exp(-\beta \Delta \mathcal{H})\}, \quad (9)$$

where $\Delta \mathcal{H}$ is the Hamiltonian's change from g to h.

Note that we assume that the system is subjected to an infinite heat bath having a "temperature" $T = 1/\beta$. We can interpret that the temperature plays a role in introducing randomness in the wiring decision because the wiring decisions become more random and insensitive to energy increases as the temperature becomes high.

The choice of Hamiltonian determines the behavior of each vertex and hence the equilibrium states. In this paper, we focus on the Hamiltonian given by

$$\mathcal{H}(g) = -\sum_{i \in V} C_i(g), \quad (10)$$

$$C_i(g) = \frac{\sum_{j,k \in R_i \cup S_i, j \neq k} \mathbf{1}_{\{(j,k) \in E\}}}{|R_i \cup S_i|(|R_i \cup S_i| - 1)}, \tag{11}$$

where $C_i(g)$ is a clustering coefficient [4] of vertex i in graph g that quantifies the ratio of the number of edges between its adjacent vertices to the number of edges that could possibly exist between them. Since the system with this Hamiltonian prefers jumping to a state with lower energy and each vertex tries to connect to a group of vertices strongly tied to each other, the resulting network topology is prone to be clustered.

In this transition process, $\Delta\mathcal{H}$ is determined locally because a clustering coefficient needs only information regarding the connection pattern of a rewiring vertex and immediately adjacent vertices. When one vertex rewires, all vertices that can contribute to $\Delta\mathcal{H}$ are at most the rewiring vertex and its adjacent vertices whose clustering coefficient changes. Intuitively, this is interpreted in such a way that a vertex can change its adjacent vertices only when all adjacent vertices as well as itself agree with the decision.

One of the intriguing properties of this model is that although the wiring decision of each vertex is made on the basis of local information, the decision could also indirectly affect the wiring decisions of other vertices that are not necessarily immediately adjacent to the vertex. The effect of one wiring-configuration change could spread over the network through a chain of reactions involving many vertices and evoke complex interactions in wiring decisions among many vertices in the whole network. Moreover the strength (length) of the interaction changes with temperature.

III. TRANSITION BETWEEN NONCLUSTERED AND HIGHLY CLUSTERED NETWORKS

In this section, we describe a Monte Carlo simulation of the aforementioned model in order to observe its equilibrium states. Following the evolution rules described in Sec. II, all vertices were given a chance to rewire their incoming edges in a round-robin manner and make a rewiring decision to a randomly selected vertex with a transition probability given by Eq. (9).

All simulations started from a randomly and independently generated random graph that contained a fixed number of vertices N and incoming degree K, and the simulation steps are chosen to be large enough (more than 16 000 steps) for the system to exhibit a long plateau in the average clustering coefficient. Note that one simulation step is defined by one "round" of turns given to all vertices for rewiring. Thus, each vertex has in total more than 16 000 opportunities for rewiring.

We used the random number generator of Kirkpatrick and Stoll [15], which has approximately a period of 2^{250} to ensure enough randomness against the scale of the simulations.

Figure 2 illustrates the average clustering coefficient of the system with $N=100$, 200, 300, 400, 600, and 800 and $K=10$ at a variety of temperatures ranging from 0.0001 to 1. The average clustering coefficient for each simulation was calculated by sampling ten different points well after the system had reached a steady state. Moreover, to eliminate the initial graph dependency, the points shown in Fig. 2 are the average clustering coefficients taken over 15 different simulations with different initial random graphs independently generated for each simulation.

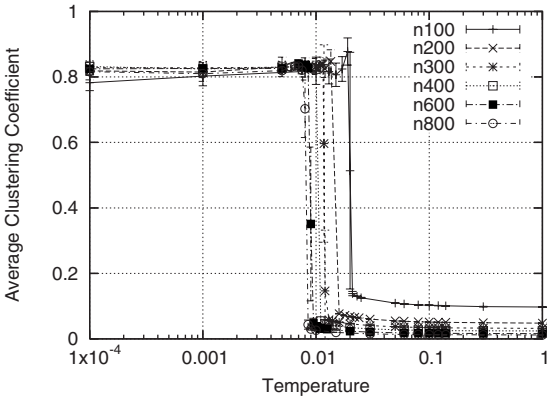

FIG. 2. Average clustering coefficients (CCs) of the system in the equilibrium states for a variety of temperatures. Error bars in the high-temperature range are smaller than the data points.

As we discussed, temperature in our model can be taken as randomness in the wiring decision. As temperature goes down, the decision becomes more and more deterministic and hence the resulting topology is prone to be more clustered. In the high-temperature limit, the network becomes a random graph because the wiring decision is made in a totally random fashion and all K 1's in the ith column of the corresponding adjacency matrix are placed randomly. (Thereby, all 1's in the adjacency matrix are equally distributed except for diagonal entries.) In the low-temperature limit, the network has a highly clustered topology with low energy. In particular, the network in the ground state contains $N/(K+1)$ isolated perfect subgraphs with $K+1$ vertices if N is dividable by $K+1$ and the average clustering coefficient takes on the maximum value, 1 (the clustering coefficient of all vertices is exactly 1). If N is not dividable by $K+1$, it is comprised of highly clustered imperfect subgraphs. Interest-

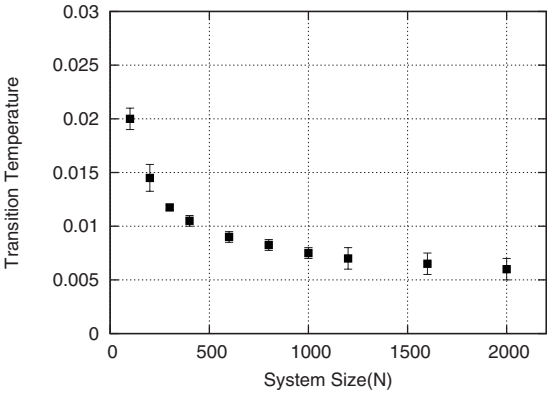

FIG. 3. Transition temperature. It is defined as the average temperature between the two consecutive simulation points having more than and less than CC=0.5 and the error bars are the temperature width between them. All simulation data for $N \geq 1000$, which were computed from only one initial topology, are also plotted to show the rough tendency of the profile.

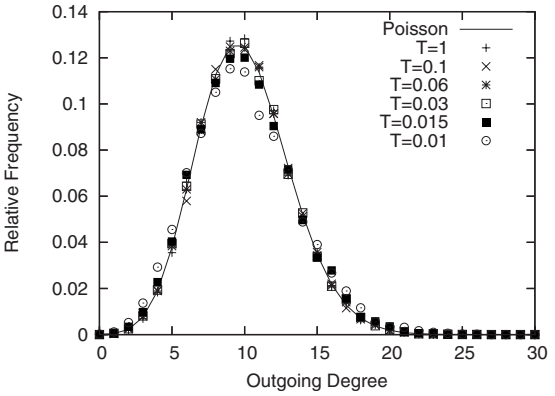

FIG. 4. Relative frequencies of outgoing degrees for $N=800$, $K=10$ at $T=1$, 0.1, 0.06, 0.03, 0.015, and 0.01. Poisson distribution ($\lambda=K$) is also plotted for comparison.

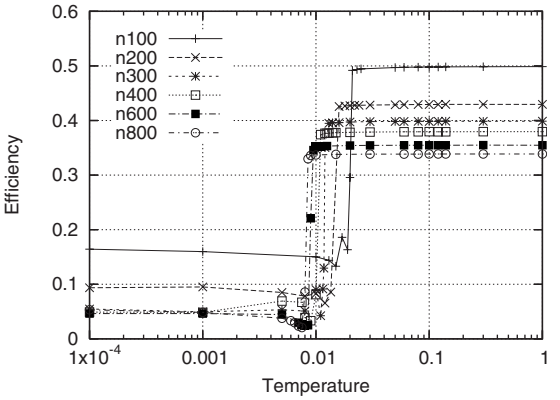

FIG. 6. Average efficiencies of networks with $N=100$, 200, 300, 400, 600, and 800.

ingly, for all system size cases, there is a sudden jump in the average clustering coefficient at a certain "critical" temperature T_c. A network with a larger N has a lower transition temperature because the degree of freedom of the system increases as N increases. Figure 3 illustrates how transition temperature decreases as the system size N increases. We can observe that the decrease in the transition temperature conspicuously becomes small as N becomes large. Note that the system is "frozen" in one of the low-energy states at a low temperature if the simulation steps are finite because once the system falls into a deep "valley" of the potential curve, the probability of transiting to other low-energy states by jumping over potential barriers is extremely small and the event practically never happens in a finite number of simulation steps.

The average clustering coefficient stays low in the high-temperature range above T_c, and this is a typical property of random graphs. Figure 4 plots the relative frequency of outgoing degrees of the network with $N=800$ at $T=1$, 0.1, 0.06, 0.03, 0.015, and 0.01 ($>T_c$). Compared to the Poisson distribution, very little difference is observed for all cases.

On the other hand, in the low-temperature range below T_c, the networks are frozen in one of the low-energy states that contain highly clustered subnetworks isolated or connected to each other with a few edges. (Figure 5 illustrates one of the typical clustered topologies observed in the case of $T=0.0001$ for $N=100$.) Figures 6 and 7 show the average efficiencies of the network [17] and the ratios of the number of disconnected vertex pairs to the number of all vertex pairs $[N(N-1)]$, respectively. These plots also show the discontinuous changes at T_c between high average efficiency (low ratio of disconnected vertex pairs) and low average efficiency (high ratio of disconnected vertex pairs), which indicates that the topologies suddenly change between connected graphs and disconnected graphs. All these results strongly suggest that topologies observed in the high-temperature range above T_c still have random graph properties and those below T_c contain multiple mutually disconnected subclusters. This jump implies a transition between a nonclustered network topology and highly clustered network and we can take the average clustering coefficient as the order parameter of the system. In our model, high temperature causes high degree of randomness in the wiring configuration, whereas low temperature causes high average clustering coefficient of the network. As the temperature drops, the randomness in the wiring decision plays a less meaningful role and the importance of the clustering coefficient grows. The critical temperature is where this balance dramatically changes and the transition between nonclustered and highly clustered networks appears. In Sec. IV, we investigate how the interaction between vertices grows above the critical temperature.

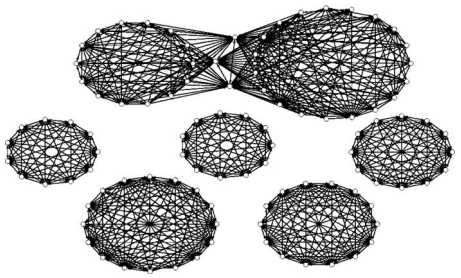

FIG. 5. Typical example of highly clustered topologies ($N=100$, $K=10$, $T=0.0001$). The graph is drawn by using PAJEK [16].

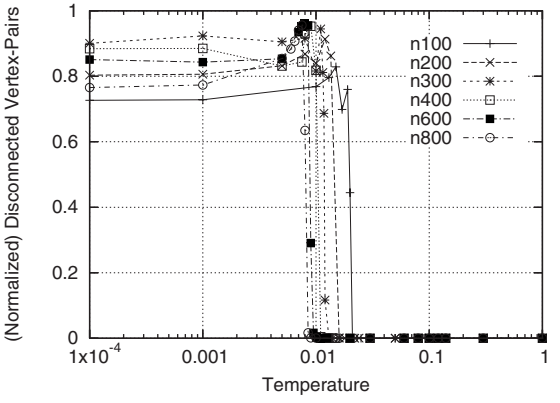

FIG. 7. The numbers of disconnected vertex pairs normalized by the whole number of possible vertex pairs for $N=100$, 200, 300, 400, 600, and 800.

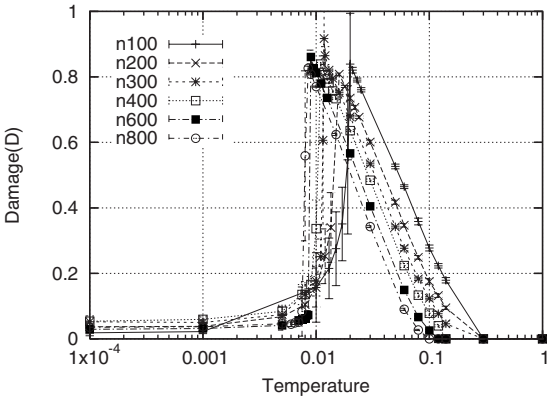

FIG. 8. Damage spreading for the same simulation set of networks in Fig. 2.

IV. HIDDEN TOPOLOGICAL STRUCTURE ABOVE THE CRITICAL POINT

The results in Sec. III imply that interactions in the wiring decision among many vertices grow above the critical point as the temperature decreases. In this section, we focus on the details of the topological structure inducing a collective reaction of the system. Such details cannot be analyzed simply with the average clustering coefficient. To this end, we take an approach commonly used in the literature on Ising models and spin glasses: damage spreading and percolation.

A. Damage spreading

Damage spreading [18,19] is a tool originally developed by Kauffman [18] to study biologically motivated dynamical systems, and it appears in the literature on Ising models and spin glasses as a way to observe the system dynamics. Damage spreading investigates the time evolution of slightly different copies of a dynamical system, which are subjected to the same thermal noise. Knowledge of whether or not a small perturbation (damage to the configuration) added to one of the two replicas diverges or stays at the same level (even disappears) can help us to investigate the interactions between vertices.

Figure 8 plots damage spreading for the same simulation set of networks shown in Fig. 2. "Damage" here is defined as a slight change in the wiring configuration of replica 2, which is a copy of the original network (replica 1). Randomly chosen and rewired are 0.5% of the edges of replica 2 so that their tail vertices are on randomly chosen. (For example, a network with $N=100$ and $K=10$ has 5 edges rewired out of 1000 edges.) Note that this operation preserves the incoming degree of all vertices. The damage is added to replica 2 in the steady state, and we compare the two replicas after leaving them to evolve in more than 8000 subsequent simulation steps. Damage spreading is defined as the ratio of the number of different edges in the edge configuration between replica 1 and replica 2 to the total number of edges (NK). The quantity D is calculated by comparing all edges of the two replicas and counting one if one edge of replica 2 consists of a different pair of vertices from the corresponding edge of replica 1:

$$D = \frac{\{\text{number of different edges}\}}{\{\text{total number of edges}\}} = \frac{\sum_{i,j} |a_{ij}^{(\text{replica 1})} - a_{ij}^{(\text{replica 2})}|}{2NK}. \quad (12)$$

Here, $a_{ij}^{(\text{replica } k)}$ denotes the (i,j) entry of the adjacency matrix of replica k ($k=1,2$), and the summation is taken over all i and j.

Figure 8 shows that damage grows as temperature decreases from a high temperature. It becomes almost 1, the maximum value, just before it reaches the critical point. Below the critical temperature, it rapidly decreases and becomes confined to a certain region. A large damage value indicates that the correlation length of the system is long, which means the wiring-configuration decision of one vertex can affect the decision of many other vertices in the network. This interaction between vertices is very complex because a variety of reaction chains (loops) would be involved in the wiring decisions of many vertices. For example, if one vertex changes its wiring configuration, it affects the decisions of the immediately adjacent vertices, which then affect their adjacent vertices, and so on. This chain reaction spreads over the network and possibly the effect of rewiring of one vertex could return to itself if the reaction chain has loops. Thus, the growth in damage implies that a complex structure is being organized and its value gives us a measure of how large the interaction region is relative to the size of the network.

These simulation results suggest the existence of a hidden complex structure regarding interaction chains stretching over many vertices above the critical temperature. In Sec. IV B, as a way of analyzing such structures, we devise a percolation expression applicable to our network model.

B. Percolation expression

1. Concept of percolation expression

Kastelayn and Fourtuin introduced the idea of percolation for analyzing the Ising spin model. Since then, percolation models have been studied in a variety of research areas. They are especially useful as a tool for understanding critical phenomena in complex statistical systems including spin glass models [20–25].

A percolation model is a system model defined by a set of local connections. In the Ising spin model, for example, an occupied bond is placed with a certain probability if two mutually adjacent vertices have the same states (spin orientations) and a vacant bond is placed otherwise. After executing this operation for all pairs of adjacent vertices (edges on a lattice grid), we get a percolation graph. Subgraphs comprised of connected vertices in the percolation graph are referred to as "percolation clusters." As we increase the probability of putting occupied bonds, a well-known phenomenon (called the percolation transition) whereby local percolation clusters suddenly combine into one macrocluster, emerges at a critical probability.

Since Kastelayn and Fourtuin's percolation expression is a strict mathematical transformation of the partition function,

we can use it as a different way of expressing the system instead of expressing it with spin orientation patterns. The percolation transition of the Ising model and the phase transition observed in the spin expression take place at the exactly same point, and we can take the distribution of percolation clusters as that of effective interaction regions of the system.

2. Percolation expression

In order to develop the percolation expression for our network model, we rewrite the Hamiltonian of our model in terms of pairs of vertices (i,j),

$$\mathcal{H}(g) = -\sum_{i \in V} C_i(g) = -\sum_{i,j} a_{ij}(g) w_{ij}(g), \tag{13}$$

where $a_{ij}(g)$ is the entry of the adjacency matrix $A(g)$. $w_{ij}(g)$, a coefficient that represents the contribution of the each pair (i,j) to the Hamiltonian, is given by

$$w_{ij}(g) = \sum_{k \in U_{ij}(g)} \frac{1}{|R_k \cup S_k|(|R_k \cup S_k| - 1)}, \tag{14}$$

where $U_{ij}(g) = (R_i \cup S_i) \cup (R_j \cup S_j)$.

Using $w_{ij}(g)$, we can express the partition function $Z(\beta)$ as follows:

$$Z(\beta) = \sum_{g \in \Sigma} \exp\{-\beta \mathcal{H}(g)\} = \sum_{g \in \Sigma} \exp\left\{\beta \sum_{i,j} a_{ij}(g) w_{ij}(g)\right\}$$
$$= \sum_{g \in \Sigma} \prod_{i,j} e^{\beta a_{ij}(g) w_{ij}(g)}. \tag{15}$$

The exponential function in the partition function can be transformed as follows:

$$e^{\beta a_{ij}(g) w_{ij}(g)} = e^{\beta w_{ij}(g)}[e^{-\beta w_{ij}(g)} + a_{ij}(g)\{1 - e^{-\beta w_{ij}(g)}\}]. \tag{16}$$

We substitute it to the partition function

$$Z(\beta) = \sum_{g \in \Sigma} \prod_{i,j} e^{\beta w_{ij}(g)}[e^{-\beta w_{ij}(g)} + a_{ij}(g)\{1 - e^{-\beta w_{ij}(g)}\}]$$
$$= \sum_{g \in \Sigma} \prod_{i,j} e^{\beta w_{ij}(g)}\{q_{ij}(g,\beta) + a_{ij}(g) p_{ij}(g,\beta)\}$$
$$= \sum_{g \in \Sigma} \prod_{i,j} e^{\beta w_{ij}(g)} \prod_{i,j} \{q_{ij}(g,\beta) + a_{ij}(g) p_{ij}(g,\beta)\}, \tag{17}$$

where

$$p_{ij}(g,\beta) = 1 - e^{-\beta w_{ij}(g)},$$

$$q_{ij}(g,\beta) = 1 - p_{ij}(g,\beta). \tag{18}$$

We can interpret the term

$$\prod_{i,j} \{q_{ij}(g,\beta) + a_{ij}(g) p_{ij}(g,\beta)\} \tag{19}$$

as a set of probability events where, for all (i,j) in a given graph g,

(1) if $a_{ij}(g)=1$, put an occupied bond with probability $p_{ij}(g,\beta)$ and put a vacant bond with probability $q_{ij}(g,\beta)$ on (i,j); and

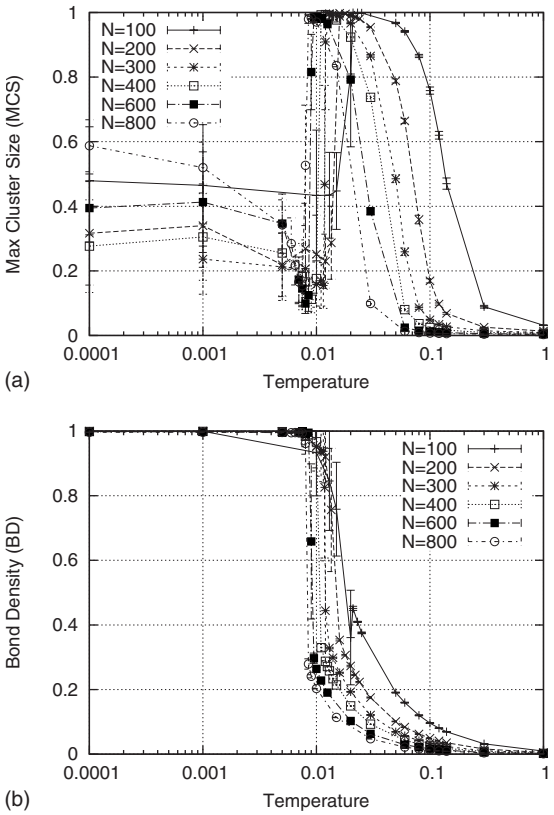

FIG. 9. Maximum cluster sizes (MCSs) and bond densities (BDs) for different system sizes N. We generated ten percolation graphs from each original network topology. Each data point represents their average. The error bars at high temperature are smaller than the data points.

(2) if $a_{ij}(g)=0$, put a vacant bond with probability of 1 on (i,j).

Then we get a percolation graph for g.

Analogously as with the percolation expression of the Ising model, we can interpret the percolation expression of our model as a graph comprised of edges representing the existence of an effective interaction between two vertices by eliminating connections created only because of thermal noise. Thereby, the percolation clusters represent the effective interaction regions.

3. Simulation results

Following the operations above, we generated percolation graphs from network topologies resulting from the network evolutions discussed in Secs. III and IV.

Figure 9 illustrate the MCSs and BDs of the percolation graphs. Here, the maximum percolation cluster size is defined as the ratio of the number of vertices in the maximum percolation cluster to N, the total number of vertices in the system, and bond density is the ratio of the number of placed effective bonds to the total number of edges. To enable comparison with the results in Secs. III and IV, we plot the results from Figs. 2, 8, and 9 for the network with $N=400$ and $K=10$ in Fig. 10.

From these figures, we can observe two distinct temperatures in terms of the states of the system. The first one is

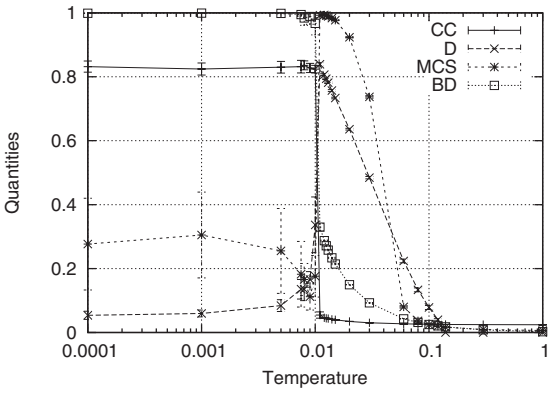

FIG. 10. Comparison between maximum cluster sizes, bond densities, and simulation results in Figs. 2, 8, and 9 for the network with $N=400$ and $K=10$.

observed by a sharp increase in MCS in a relatively high temperature range (around $T\sim0.05$). We call this point as a percolation transition temperature T_p. Above T_p, both MCS and BD stay low and below T_p on the other hand, MCS reaches almost up to 1 and BD still stays low and shows moderate increase.

The second one is observed by a sudden decrease in MCS and a sudden increase in BD. We can see it at around $T\sim0.01$. This point coincides with T_c at which the network takes a clustered topology and D plummets. Below T_c, MCS stays relatively small, in contrast to BD and CC, which take large values.

We interpret that MCS indicates the dominant interaction region in the system because it represents the domain connected by effective bonds, which are placed on "meaningful" edges whose contribution to the Hamiltonian is large. In the high-temperature region, MCS and BD stay low because most of the edges are randomly created and a rewiring decision of one vertex does not affect other vertices' decision for next rewiring. (Thus the graph is pretty sparse and random, and the correlation length is short.) As the temperature decreases, BD, which reflects the number of deterministically created edges, gradually increases and MCS suddenly jumps at T_p. Considering that the original graphs in this temperature region show random graph properties, we can take T_p as the transition temperature at which most of the vertices are suddenly connected to each other with meaningful edges in the same way as observed in random graphs.

In the intermediate-temperature region ($T_c<T<T_p$), high values of MCS and D indicate that the interaction region is stretched over the whole network. Note that D also starts increasing around T_p, and MCS and D have strong positive correlation. Percolation analysis is basically a static method used to analyze the interaction region in terms of contributions to the Hamiltonian in contrast to damage spreading, a dynamic method that depends on simulation dynamics. Both different ways indicate that T_p is the boundary at which the interaction region starts spreading. As the temperature approaches T_c, BD shows an accelerated increase even though the average clustering coefficient still stays low. Since BD indicates the ratio of deterministically placed (meaningful) edges to all edges, this result implies that once a certain number of edges are deterministically placed, possible wiring-configuration patterns are suddenly limited and the topological structure (clustered graph) rapidly grows through the interaction. Then, as we previously discussed in Sec. III, topologies suddenly transit from random graphs to highly clustered graphs at T_c. In that sense, percolation graph reveals a "hidden" yet growing structure by "filtering" the original graph and eliminating thermally fluctuating edges. This sudden growth of BD implies that a positive feedback effect through complex reaction chains among vertices appears in such a way that the structure generated by one meaningful wiring attracts previously meaningless edges (connections due to thermal fluctuation) and induces more structure and so forth just above T_c.

Finally, below T_c, the network becomes divided into subclusters, MCS is bounded by the maximum size of the subclusters, and D is confined to within the clusters. Moreover, BD reaches almost 1, which means almost all edges become meaningful because of the transition to a highly clustered structure, and percolation graphs become identical to the original ones.

V. DISCUSSION AND CONCLUSION

We developed a network model similar to the Ising model that involves statistical mechanics for studying the equilibrium states of network evolutions where vertices autonomously keep changing their wiring configuration according to the locally defined metric. Taking the clustering coefficient as a metric for structuring networks, we analyzed the temporal evolution and the network topology in the equilibrium states by performing Monte Carlo simulations.

Our simulation results showed the transition temperature at which a sudden jump in the average clustering coefficient of the system is observed. The simulation results of other network properties such as average efficiency and the number of disconnected vertex pairs also indicate that the sudden topological transition between random graphs and highly clustered graphs happens at this temperature.

In order to see the details of how this transition happens, we performed damage spreading and percolation analysis to observe the interaction region among vertices. The damage-spreading simulation told us that interactions between vertices stretch over the whole network and two slightly different replicas take totally different trajectories in a phase space slightly above T_c.

Percolation expression applicable to our model observed two distinct temperatures T_p and T_c in the maximum cluster size of the percolation graph, which indicates an interaction region in the network, and bond density, which indicates the ratio of effective (deterministically placed) edges. The maximum cluster size jumps at T_p and shows a strong positive correlation with damage spreading. The sudden increase in bond density coincides with the transition between a nonclustered topology and a highly clustered topology at T_c.

All these results support the idea that some structure (complex interactions between vertices) that cannot be revealed by the average clustering coefficient grows above the critical point. Since the bond density indicates the ratio of

deterministically placed (meaningful) edges to the total edges, this result implies that once a certain number of edges are deterministically placed and create a certain structure, most of the edges suddenly become meaningful and the topological structure (clustered graph) rapidly grows through the interaction. In that sense, percolation graph reveals a hidden yet growing structure by filtering the original graph and eliminating thermally fluctuating edges. This sudden growth of BD implies that a positive feedback effect through complex reaction chains among vertices appears in such a way that the structure generated by one meaningful wiring attracts previously meaningless edges (connections due to thermal fluctuation) and induces more structure and so forth just above T_c.

This paper mainly discussed the transition by formalizing a model of networks with evolving wiring structure. However, there are still lots left to be studied. For future work, more extensive analysis (for example, finite-size scaling) is necessary to understand the behavior of the system, in particular, at around the distinct temperatures. An analytical derivation should be also developed.

Moreover, we can extend the model in various ways by introducing protocols for wiring operations to model applications in real networks. For instance, vertices might be allowed to "reject" being connected to other vertices. The weights of edges should be considered if we want to differentiate the edges' importance. Furthermore, by taking into account physical parameters such as available bandwidth and traffic demand between vertices, for example, our model could be applied to more realistic applications. We believe that our model is a step toward many fruitful research topics.

ACKNOWLEDGMENTS

The authors thank Michihiro Kandori, Balaji Prabhakar, and Andrea Goldsmith for their help and exciting conversations.

[1] P. Erdos and P. Renyi, Publ. Math. (Debrecen) **6**, 290 (1959).
[2] P. Erdos and P. Renyi, Publ. Math. Inst. Hung. Acad. Sci. **5**, 17 (1960).
[3] P. Erdos and P. Renyi, Bull. Internat. Statist. Inst. **38**, 343 (1961).
[4] D. J. Watts and S. H. Strogatz, Nature (London) **393**, 440 (1998).
[5] D. J. Watts, *Small Worlds: The Dynamics of Networks between Order and Randomness* (Princeton University Press, Princeton, NJ, 2003).
[6] S. Milgram, Psychol. Today **2**, 60 (1967).
[7] A. L. Barabasi and R. Albert, Science **286**, 509 (1999).
[8] M. E. J. Newman, SIAM Rev. **45**, 167 (2003).
[9] R. Albert and A. L. Barabasi, Rev. Mod. Phys. **74**, 47 (2002).
[10] S. Boccaletti, Phys. Rep. **424**, 175 (2006).
[11] S. H. Strogatz, Nature (London) **410**, 268 (2001).
[12] M. E. J. Newman, in *Handbook of Graphs and Networks*, edited by S. Bornholdt and H. G. Schuster (Wiley-VCH, Berlin, 2003).
[13] M. Talagrand, *Spin Glasses: A Challenge For Mathematicians—Cavity and Mean Field Models* (Springer, New York, 2003), Vol. 46.
[14] N. Metropolis, A. W. Rosenbluth, M. N. Rosenbluth, A. H. Teller, and E. Teller, J. Chem. Phys. **21**, 1087 (1953).
[15] S. Kirkpatrick and E. P. Stoll, J. Comput. Phys. **40**, 517 (1981).
[16] http://vlado.fmf.uni-lj.si/pub/networks/pajek/
[17] V. Latora and M. Marchiori, Eur. Phys. J. B **32**, 249 (2003).
[18] S. A. Kauffman, J. Theor. Biol. **22**, 437 (1969).
[19] M. L. R. Puzzo and E. V. Albano, Comm. Comp. Phys. **4**, 207 (2008).
[20] P. W. Kasteleyn and C. M. Fortuin, J. Phys. Soc. Jpn. **26**, 11 (1969).
[21] C. M. Fortuin and P. W. Kasteleyn, Physica (Amsterdam) **57**, 536 (1972).
[22] A. Coniglio and W. Klein, J. Phys. A **13**, 2775 (1980).
[23] Y. Kasai and A. Okiji, Prog. Theor. Phys. **79**, 1080 (1988).
[24] H. Imaoka, H. Ikeda, and Y. Kasai, Physica A **246**, 18 (1997).
[25] I. A. Campbell and L. Bernardi, Phys. Rev. B **50**, 12643 (1994).